Effect of Al on the solid reaction between $3CaO \cdot Al_2O_3$ oxide and Fe-S-O-Al alloy at 1373 K

Authors:

Dr. Yi Wang
Lecturer at School of Metallurgical and Ecological Engineering, University of Science and Technology Beijing (USTB), Beijing 100083, China
Email: wangyi@metall.ustb.edu.cn

Prof. Lifeng Zhang (Correspondence Author)
Professor at State Key Laboratory of Metastable Materials Science and Technology, School of Mechanical Engineering, Yanshan University, Qinhuangdao City, Hebei Province 066004, China
Email: zhanglifeng@ysu.edu.cn
Phone number: 86-0335-8074666

Prof. Ying Ren (Correspondence Author)
Professor at School of Metallurgical and Ecological Engineering, University of Science and Technology Beijing (USTB), Beijing 100083, China
Email: yingren@ustb.edu.cn

Dr. Zushu Li
Reader at Advanced Steel Research Centre, WMG, University of Warwick, Coventry, CV4 7AL, U.K.
Email: z.li.19@warwick.ac.uk

Abstract: Diffusion couples of $3CaO \cdot Al_2O_3$ and Fe-S-O-(Al) alloys were prepared to investigate the transformation of calcium aluminate reacting with solid sulfur-containing alloys. Diffusion behaviors and solid reaction between the alloy phase and the slag phase under 1373 K were studied. Product layers of $12CaO \cdot 7Al_2O_3$ and CaS were formed at the interface. After heating for 10 h, the average thickness of CaS layer in samples with and without Al in the alloy phase was 2.10 μm and 0.71 μm, respectively, while it increased to 3.76 μm and 1.75 μm after 50 h heating. Aluminum in the alloy made the solid reaction at the interface easier to happen, meanwhile inhibited the formation of CaS layer by promoting the formation of $12CaO \cdot 7Al_2O_3$ layer and suppressed the diffusion of sulfur.

Keywords: diffusion couple, solid reaction, $3CaO \cdot Al_2O_3$, Fe-S-O-Al alloy, desulfurization

1. Introduction

During the production of Al-killed steels, alumina inclusions were modified to calcium aluminate by Ca treatment or slag-steel interaction[1-3] to reduce the adverse effect on the steel quality caused by the nozzle clogging or poor deformability of inclusions[4-7]. The formation of CaS occurred in both liquid[8, 9] and solid steels[10, 11], resulting in defects of steel products like pittings[12]. Shin et al. verified the participation of Al during the formation of CaS in the liquid steel following the reaction of $2[Al]+3[S]+3(CaO)=(Al_2O_3)+3(CaS)$[13]. The CaS also precipitated in the solid steel. Kitamura et al. reported the formation of CaS in the solid steel due to the solid reaction between the calcium aluminate and the ultra-low sulfur steel during the heat treatment process[14].

Solid reactions between inclusions and alloys during heat treatments under 1273 to 1623 K have been widely studied, including the systems of Fe-Mn-Si alloy and $MnO-SiO_2-(FeO)$ slag[15-17], Fe-Al-Ca alloy and Al_2O_3-CaO-(FeO) slag[18-20], etc. Effects of the composition, temperature, and time on the solid reaction have been discussed, which mainly focused on the effect of S on the diffusion of O, rather than the formation of CaS[21]. Kim et al. measured the solubility of sulfur in various calcium aluminates[22]. Baba brought this study further into the metal-slag system[23]. Their study verified that the formation of CaS around $12CaO\cdot7Al_2O_3$ particles was suppressed by the diffusion of sulfur in the solid oxide. However, Al, as an element coexisting with calcium aluminate inclusions in Al-killed steels, its effect on CaS formation during the solid reaction was rarely reported.

In the current study, diffusion couples were used to investigate the effect of Al on the element diffusion and solid reaction between Fe-S-O-(Al) alloys and the $3CaO\cdot Al_2O_3$ slag under 1373 K.

2. Experimental

The slag of $3CaO\cdot Al_2O_3$ was prepared using CaO and Al_2O_3 powders of reagent pure grade. Powders of CaO and Al_2O_3 with a molar ratio of 3:1 were put into a graphite crucible and melted at 1873 K for 1 h in a resistance furnace. The melting process was repeated twice to obtain a homogenous slag composition. After grinding, the slag was heated at 1273 K for 10 h in a muffle furnace for decarburization. To prepare the alloy of Fe-S-O-Al, 500 g electrolytic iron was put into an alumina crucible and melted in a resistance furnace at 1873 K under an Ar atmosphere. After holding for 15 min, 0.25 g sulfur was added into the liquid iron. Five minutes later, the sample Alloy-A was taken from the crucible using a quartz tube sampler. Then 0.1 g Fe_2O_3 was put into the crucible, followed by 0.4 g Al with a time interval of 5 min. Another 5 min later, sample Alloy-B was taken by a quartz tube sampler. The total oxygen content (T.O) and total sulfur content (T.S) in alloy samples were analyzed using Leco ONH836 and Leco CS844. The acid soluble aluminum (Al_s) was analyzed using the inductively coupled plasma method. The composition of alloy samples was listed in **Table 1**. The Al_s in Alloy-A was brought

in as an impurity of the electrolytic iron. The content of Al_s in Alloy-A was quite low that it could be ignored.

Table 1 Composition of alloy samples

Sample	T.O (ppm)	T.S (ppm)	Al_s (wt%)	Fe
Alloy-A	138	571	0.0004	Bal.
Alloy-B	128	540	0.0610	Bal.

Alloy samples were cut into cylinders with a size of Φ5 mm x 3 mm. A hole was drilled in the center of each cylinder using a Φ1 mm drill. After derusting with a grinding wheel and ultrasonic cleaning in the ethanol, holes in alloy cylinders were filled with the $3CaO{\cdot}Al_2O_3$ (C_3A) slag to make diffusion couples of the $3CaO{\cdot}Al_2O_3$ slag and Fe-S-O-(Al) alloys. Using a high-temperature confocal laser scanning microscopy (CLSM), diffusion couples were first heated to 473 K with a rate of 50 K/min, then to 1723 K by 800 K/min and holding for a few seconds, followed by He gas quenching immediately after the slag phase was melted. Diffusion couples were sealed in quartz tubes which were filled with Ar gas. A piece of Ti foil was put into each quartz tube to prevent the oxidation of samples. Quartz tubes with diffusion couples inside were put into a muffle furnace, the temperature inside which was increased to 1373 K with a rate of 10 K/min. After holding at 1373 K for 10 h, quartz tubes were quenched with water. Diffusion couples inside these tubes were named as A-10 and B-10. Samples quenching after holding at 1373 K for 50 h were named as A-50 and B-50. Samples without heat treatment were named as A-0 and B-0. All these samples were mounted with epoxy and polished for the observation of the interface between the slag phase and the alloy phase. A Scanning Electron Microscope and an Energy Dispersive Spectrometer were used for the interface analysis.

3. Results and discussion

Fig. 1 shows the morphology and element distribution near the interface between the slag phase and the alloy phase of samples A-0 and B-0. The left side with light color was the alloy phase, while the dark phase on the right side was the slag. Near the interface, the diffusion of elements had slightly taken place before the heat treatment. The mass ratio of Ca and Al (Ca/Al) in the bulk phase of slag was about 2.22, closed to the value of $3CaO{\cdot}Al_2O_3$. The mass ratio of Ca/Al increased from the bulk phase of slag to the interface for sample A-0. For sample B-0 with 0.0610% Al in the alloy phase, the mass ratio of Ca/Al decreased near the interface from the bulk slag.

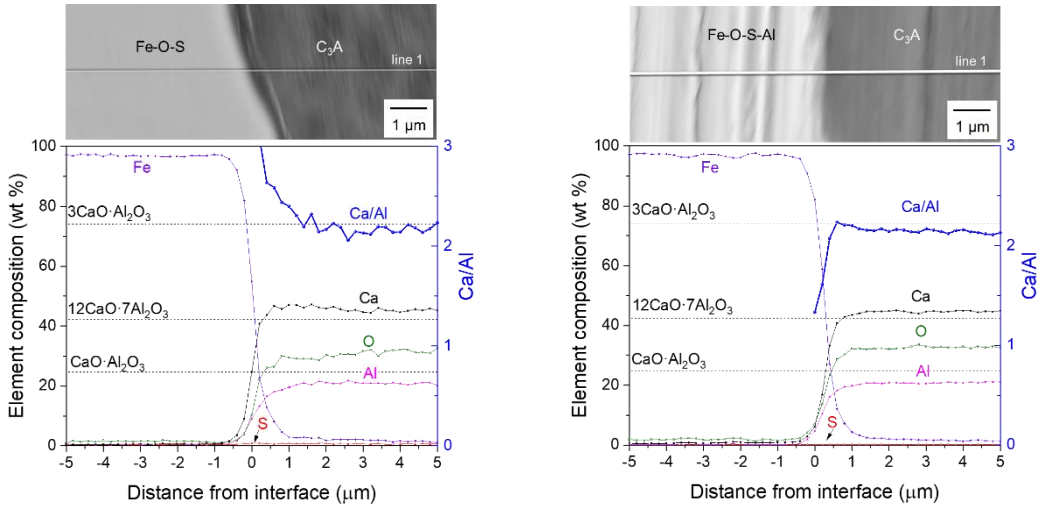

(a) (b)

Fig. 1. Morphology and element composition near the alloy-slag interface of (a) sample A-0, and (b) B-0 before the heat treatment

The alloy-slag interfaces of samples A-10 and B-10 were shown in **Fig. 2**. After heating at 1373 K for 10 h, a new phase with a color of light grey was clearly observed between the slag phase and the alloy phase, the composition of which was verified as CaS by the element distribution of Ca and S near the interface. The average thicknesses of the CaS layer in samples A-10 and B-10 were 0.71 μm and 2.10 μm, respectively. The formation of CaS layer indicated that the transformation of calcium aluminate inclusions from CaO to CaS not only occurred during the solidification process of the liquid steel but also during the cooling process of the solid steel. It was noticed that there was a new layer of calcium aluminate with dark color formed between CaS layer and the bulk phase of slag in sample B-10. The composition was close to $12CaO \cdot 7Al_2O_3$. Its average thickness was 4.84 μm.

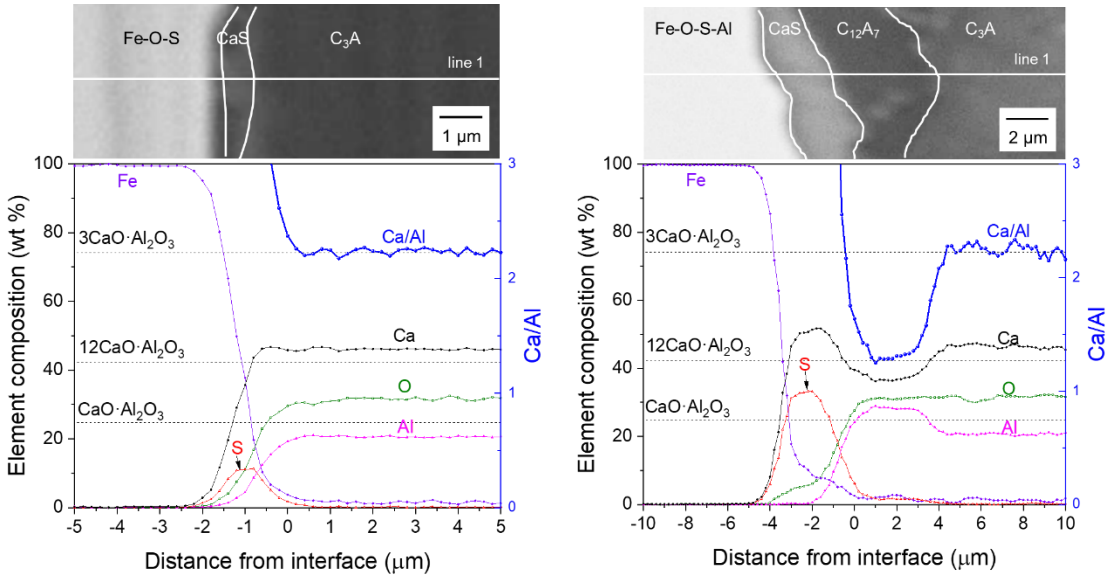

(a) (b)

Fig. 2. Morphology and element composition near the alloy-slag interface of (a) sample

A-10, and (b) B-10 after heating at 1373 K for 10 h

The morphology, element distribution, and element mapping near the interface of samples A-50 and B-50 are illustrated in **Fig. 3** and **Fig. 4**. After heating at 1373 K for 50 h, the multiple layers structure similar to sample B-10 was also observed in sample A-50, while for sample B-50, there was an extra layer of CaS generated between the $12CaO{\cdot}7Al_2O_3$ phase and the $3CaO{\cdot}Al_2O_3$ phase. The gap between the Fe-O-S-Al alloy and CaS layer was probably generated by cooling shrinkage during quenching, as the adjacent phases of both the CaS and the steel matrix had big expansion coefficients[24]. The average thicknesses of CaS layer between the alloy and the $12CaO{\cdot}7Al_2O_3$ were 1.75 μm and 3.76 μm for samples A-50 and B-50, respectively. The average thicknesses of $12CaO{\cdot}7Al_2O_3$ layer were 13.36 μm and 14.58 μm respectively.

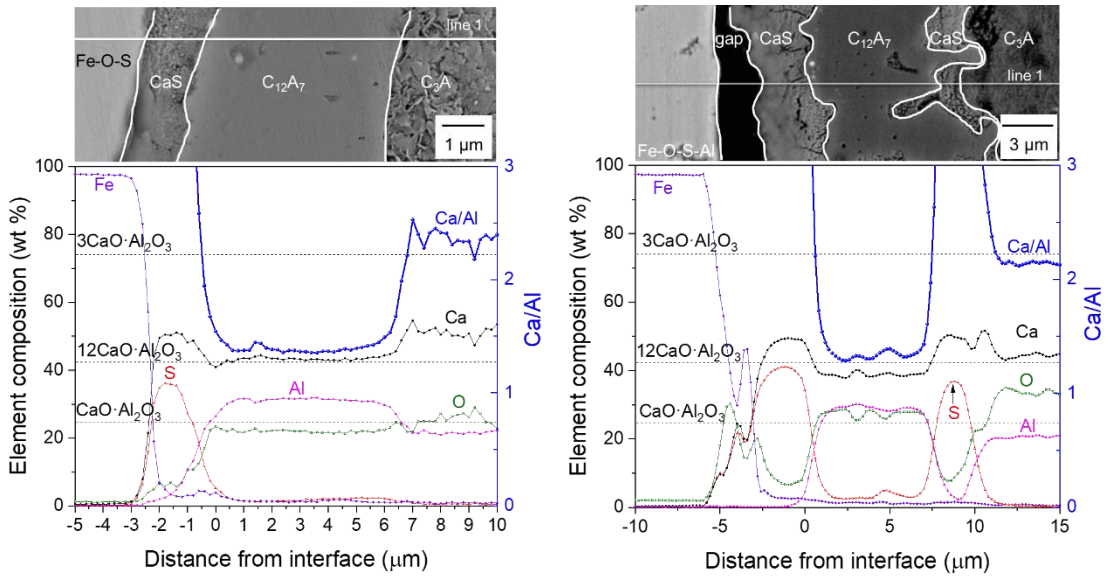

(a) (b)

Fig. 3. Morphology and element composition near the alloy-slag interface of (a) sample A-50, and (b) B-50 after heating at 1373 K for 50 h

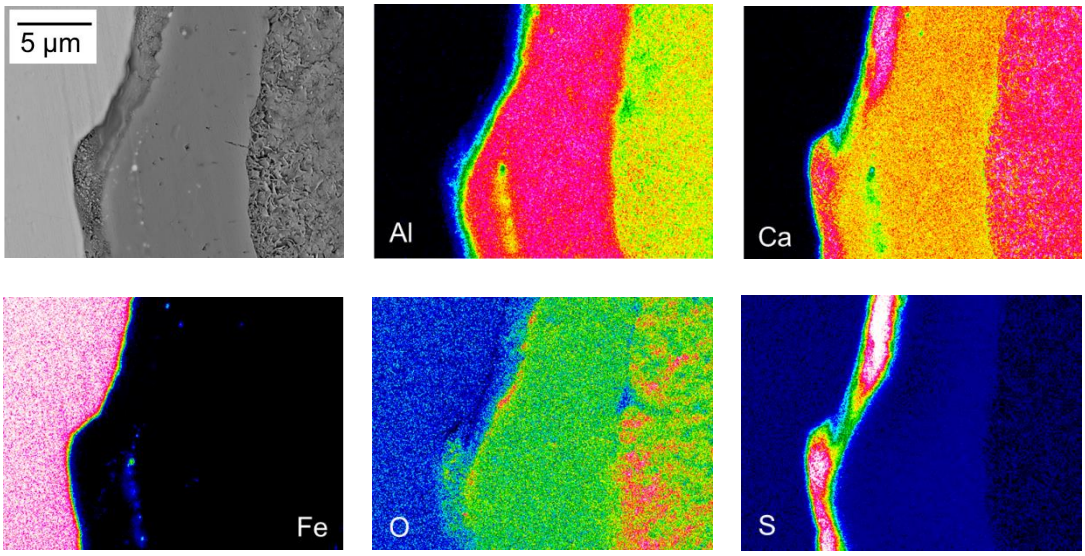

(a)

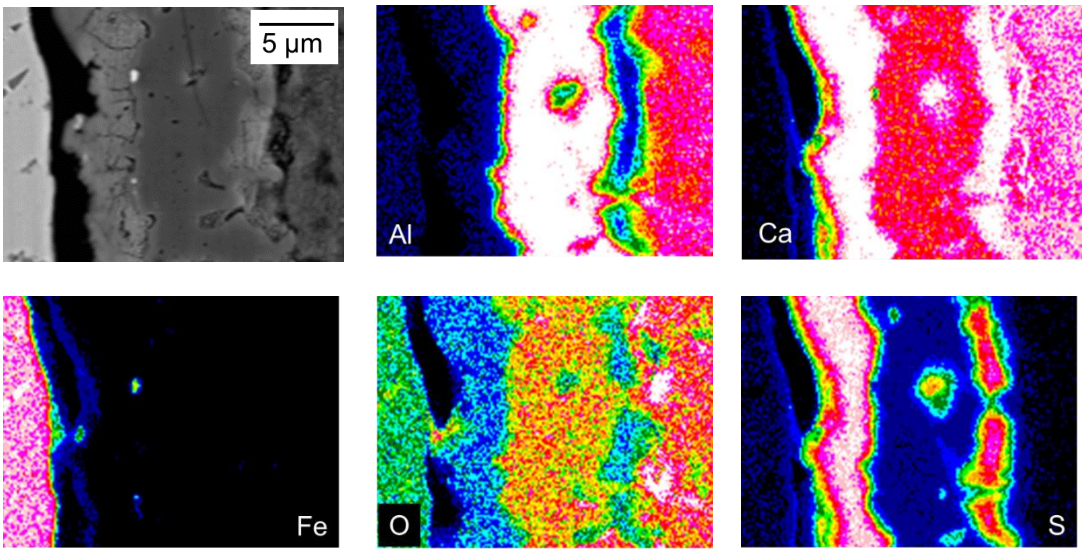

(b)

Fig. 4. Element mapping of the alloy-slag interface of (a) sample A-50, and (b) B-50

For diffusion couples made of the alloy without Al, the layer of $12CaO \cdot 7Al_2O_3$ was formed during the heat treatment due to the diffusion of Ca. Though no $12CaO \cdot 7Al_2O_3$ layer was observed in sample A-0, the mass ratio of Ca/Al in the slag phase increased toward the slag-alloy interface, indicating the diffusion of Ca from the slag phase to the alloy. After the heat treatment of 10 h, a thin layer of CaS was formed at the interface as Ca and S diffused from the slag phase and the alloy met at the interface. As the diffusion and solid reaction proceeded, $12CaO \cdot 7Al_2O_3$ layer was observed in sample A-50 due to the depletion of Ca. The solid reaction between Fe-S-O alloy and $3CaO \cdot Al_2O_3$ was as follow:

$$7(3CaO \cdot Al_2O_3)+9Fe+9S=12CaO \cdot 7Al_2O_3+9CaS+9FeO \quad (1)$$

For the alloy phase containing Al, the formation of $12CaO \cdot 7Al_2O_3$ was by the opposite diffusion of Al from the alloy and Ca from the slag phase. Before the heat treatment, though little $12CaO \cdot 7Al_2O_3$ layer was detected, the mass ratio of Ca/Al in the slag phase decreased toward the slag-alloy interface, indicating the diffusion rate of Al in the alloy was faster than that of Ca in the slag phase. Both CaS layer and $12CaO \cdot 7Al_2O_3$ layer appeared in sample B-10. The position of $12CaO \cdot 7Al_2O_3$ was between the slag phase and CaS layer. The first reason was that it was difficult for S to transfer through $12CaO \cdot 7Al_2O_3$ layer, which would be discussed in the following part. Besides, the $12CaO \cdot 7Al_2O_3$ caused by depletion of Ca was adjacent to the bulk slag. As the heating time increased to 50 h, the thicknesses of product layers of CaS and $12CaO \cdot 7Al_2O_3$ increased. The solid reaction between the Fe-S-O-Al alloy and $3CaO \cdot Al_2O_3$ is shown in Eq. (2).

$$11(3CaO \cdot Al_2O_3)+6Al+9S=2(12CaO \cdot 7Al_2O_3)+9CaS \quad (2)$$

Gibbs free energies of Reactions (1) and (2) at 1373 K were calculated[16, 25, 26]. Parameters give in Reference 16 and 25 were for liquid steel temperature but assumed that they could be extended to 1373 K. The changes of Gibbs free energy of Reactions (1) and (2) were -

276664.1 J/mol and -1809621.5 J/mol respectively. It indicated that Reactions (1) and (2) could happen under 1373 K and the latter was easier to happen than the former one.

Yang's study[27] showed that the positively charged lattice framework $[Ca_{24}A_{28}O_{64}]^{4+}$ of $12CaO{\cdot}7Al_2O_3$ was compensated for by anions accommodated within the nanocages. In the current study, after diffusing from the Fe-S-O-(Al) alloy to the product layer of $12CaO{\cdot}7Al_2O_3$, atoms of S reacted with the oxygen radicals (O^{2-}, O^-, O_2^-, O_2^{2-}), which were formerly entrapped in the nanocages of $[Ca_{24}A_{28}O_{64}]^{4+}$ in $12CaO{\cdot}7Al_2O_3$ by giving them electrons. The anions of S^{2-} were entrapped by these nanocages, while the diffusion of Al and Ca were barely affected. Therefore, as Al in the alloy phase made the formation of $12CaO{\cdot}7Al_2O_3$ layer easier, the diffusion of S was inhibited, and the formation rate of CaS decreased.

However, the thicknesses of CaS layer in samples B-10 and B-50 were thicker than those in samples A-10 and A-50, respectively. The effect of Al in the alloy on the amount of the product CaS, as well as the mass fractions of element in the alloy phase under equilibrium at 1373 K was calculated by FactSage 7.0. The mass ratio of the slag phase and alloy phase used in the thermodynamic calculation were estimated based on the diffusion coefficient of Ca in the slag and the diffusion coefficient of S in the solid steel at 1373 K[28, 29]. The results are shown in **Fig. 5**. When the Al content in the alloy phase increased from zero to around 0.05 %, the precipitation of CaS increased, as well as the diffusion of S from the alloy and Ca from the slag to the interface. After that, with higher Al content in the alloy, the precipitation of CaS was constant under equilibrium. At the equilibrium state under 1373 K, more CaS was precipitated in the diffusion couple made with Alloy B than that made with Alloy A. Comparing to the diffusion of Ca in Fe-S-O and $3CaO{\cdot}Al_2O_3$ system, Al in Fe-S-O-Al alloy could also promote the formation of the product layer of CaS. Taking both the inhibiting and promoting effect of Al in the alloy into consideration, the formation mechanism of the multiple layer structure during the heat treatment is shown in **Fig. 6**.

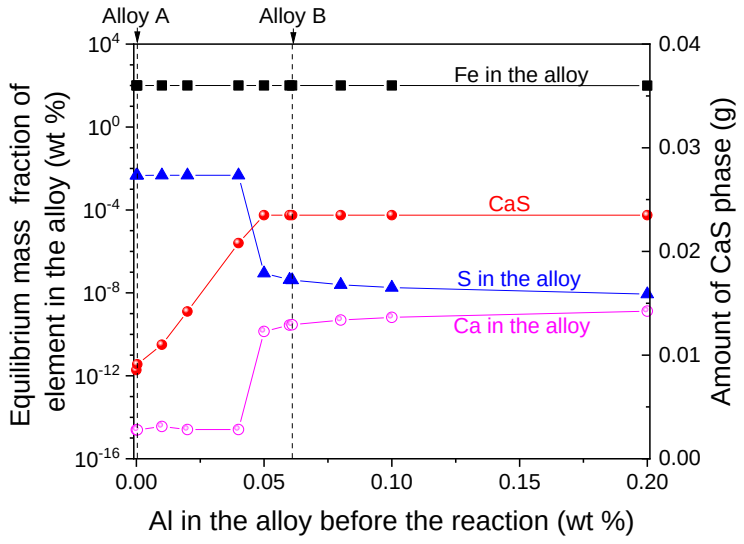

Fig. 5. Diffusion of elements and formation amount of CaS calculated by FactSage 7.0

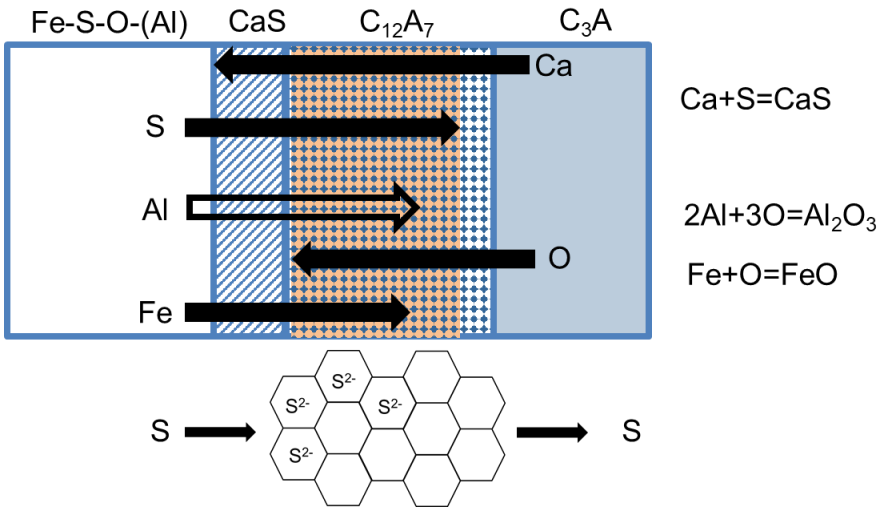

Fig. 6. Formation mechanism of the multiple layer structure during the heat treatment

4. Conclusions

1) The solid reaction between the $3CaO·Al_2O_3$ and Fe-S-O-(Al) occurred under 1373 K. The formation of CaS verified that the transformation of calcium aluminate inclusions from CaO to CaS not only happened during the solidification process of liquid steel but also by solid reaction during the cooling and heat treatment process.
2) For the solid reaction between $3CaO·Al_2O_3$ and Fe-S-O, the formation of $12CaO·7Al_2O_3$ was the results of the diffusion of Ca and the solid reaction at the interface as follow: $7(3CaO·Al_2O_3)+9Fe+9S=12CaO·7Al_2O_3+9CaS+9FeO$.
3) For the solid reaction between $3CaO·Al_2O_3$ and Fe-S-O-Al, $12CaO·7Al_2O_3$ formed due to the opposite diffusion of Al and Ca. The reaction formula was $11(3CaO·Al_2O_3)+6Al+9S=2(12CaO·7Al_2O_3)+9CaS$.
4) Aluminum in the alloy promoted the solid reaction at the interface. Under the same condition of the heat treatment, the product layer of CaS and $12CaO·7Al_2O_3$ was thicker in diffusion couples made of Fe-S-O-Al than those of Fe-S-O. Meanwhile, Al in the alloy also had an inhibiting effect on the formation of CaS layer, as the positively charged nanocages in the crystal lattice of $12CaO·7Al_2O_3$ inhibited the diffusion of S.

Declaration of competing interest

The authors declare that they have no known competing financial interests or personal relationships that could have appeared to influence the work reported in this paper.

Acknowledgements

The authors are grateful for support from the National Natural Science Foundation of China (Grant No. U1860206, No. 51725402, No. 51874032), S&T Program of Hebei (Grant No.20311004D, 20591001D), the High Steel Center (HSC) at Yanshan University and University of Science and Technology Beijing, and Beijing International Center of Advanced and Intelligent Manufacturing of High Quality Steel Materials (ICSM) at

University of Science and Technology Beijing (USTB), China.

References

[1] L. Holappa, M. Hamalainen, M. Liukkonen, M. Lind, Ironmak. Steelmak. 2002, 30, 111.

[2] Z. W. Hou, M. Jiang, E. J. Yang, S. Y. Gao, X. H. Wang, Metall. Mater. Trans. B, 2018, 49, 3056.

[3] S. Zhao, S. P. He, G. J. Chen, M. M. Peng, Q. Wang, Ironmak. Steelmak. 2014, 41, 153.

[4] Z. Y. Deng, M. Y. Zhu, Y. L. Zhou, S. C. Du, Metall. Mater. Trans. B, 2016, 47, 2015.

[5] L. F. Zhang, Y. F. Wang, X. J. Zuo, Metall. Mater. Trans. B, 2008, 39, 534.

[6] Y. T. Guo, S. P. He, G. J. Chen, Q. Wang, Metall. Mater. Trans. B, 2016, 47, 2549.

[7] Q. Ren, W. Yang, L. Cheng, L. F. Zhang, A. N. Conejo, Metall. Mater. Trans. B, 2020, 51, 200.

[8] N. Verma, P. C. Pistorius, R. J. Fruehan, M. Potter, S. R. Story, Metall. Mater. Trans. B, 2011, 42, 720.

[9] Y. Higuchi, M. Mumata, S. Fukagawa, K. Shinme, ISIJ Int. 1996, 36, S151.

[10] Y. P. Chu, W. F. Li, Y. Ren, L. F. Zhang, Metall. Mater. Trans. B, 2019, 50, 2047.

[11] Q. Ren, Y. X. Zhang, Y. Ren, L. F. Zhang, J. J. Wang, Y. D. Wang, J. Mater. Sci. Technol. 2021, 61, 147.

[12] G. Wranglen, Corros. sci. 1974, 14, 331.

[13] J. H. Shin, J. H. Park, Metall. Mater. Trans. B, 2018, 49, 311.

[14] S. Kitamura, in Proceedings of VII International Conference on Molten Slags Fluxes and Salts, The South African Institute of Mining and Metallurgy, Johannesburg, South Africa, 2004, 769.

[15] K. H. Kim, S. J. Kim, H. Shibata, S. Y. Kitamura, ISIJ Int. 2014, 54, 2144.

[16] C. S. Liu, K. H. Kim, S. J. Kim, J. S. Li, S, Ueda, X. Gao, H. Shibata, S. Y. Kitamura, Metall. Mater. Trans. B, 2015, 46, 1875.

[17] X. L. Zhang, S. F. Yang, C. S. Liu, J. S. Li, Q. Liu, G. Liu, J. Iron Steel Res. Int. 2018, 25, 1.

[18] C. S. Liu, S. F. Yang, J. S. Li, H. W. Ni, X. L. Zhang, Metall. Mater. Trans. B, 2017, 48, 1348.

[19] C. S. Liu, H. Zhang, X. Q. Liu, F. Ye, JOM, 2019, 71, 1793.

[20] C. S. Liu, S. F. Yang, J. S. Li, H. W. Ni, X. L. Zhang, Metals, 2017, 7, 129.

[21] C. S. Liu, S. F. Yang, K. H. Kim, J. S. Li, H. Shibata, S. Y. Kitamura, Int. J. Min. Met. Mater. 2015, 22, 811.

[22] S. J. Kim, M. Kageyama, X. Gao, S. Ueda, S. Y. Kitamura, ISIJ Int. 2019, 59, 1752.

[23] Y. Baba, X. Gao, S. Ueda, S. Y. Kitamura, ISIJ Int. 2020, 60, 1617.

[24] N. Anmark, A. Karasev, P. JoNsson, Mater. 2015, 8, 751.

[25] H. Suito, R. Inoue, ISIJ Int. 1996, 36, 528.

[26] J. PirajAin, Thermodynamics-Interaction Studies-Solids, liquids and gases, InTech, Rijeka, 2011.

[27] S. Yang, J. N. Kondo, K. Hayashi, M. Hirano, K. Domen, H. Hosono, Chem. Mater. 2004, 35, 104.

[28] K. C. Mills, Slag Atlas (2nd Ed.), Verlag Stahleisen GmbH, Düsseldorf, 1995.

[29] L. Gui, M. Long, S. Wu, Z. Dong, D. Chen, Y. Huang, H. Duan, L. Vitos, J. Mater. Sci. Tech. 2019, 35, 2383.

CAPTIONS:

LIST OF TABLES

LIST OF FIGURES

Table 1 Composition of alloy samples

Sample	T.O (ppm)	T.S (ppm)	Al_s (wt%)	Fe
Alloy-A	138	571	0.0004	Bal.
Alloy-B	128	540	0.0610	Bal.